Biochimica et Biophysica Acta 1818 (2012) 2126–2134

Contents lists available at SciVerse ScienceDirect

Biochimica et Biophysica Acta

journal homepage: www.elsevier.com/locate/bbamem

Ato protein interactions in yeast plasma membrane revealed by fluorescence lifetime imaging (FLIM)

Dita Strachotová [a,b], Aleš Holoubek [b,1], Helena Kučerová [a,b], Aleš Benda [c], Jana Humpolíčková [c], Libuše Váchová [a], Zdena Palková [b,*]

[a] Institute of Microbiology of the ASCR, v.v.i., Vídeňská 1083, 142 20 Prague 4, Czech Republic
[b] Department of Genetics and Microbiology, Faculty of Science, Charles University in Prague, Viničná 5, 128 44 Prague 2, Czech Republic
[c] J. Heyrovský Institute of Physical Chemistry of the ASCR, v. v. i., Dolejškova 3, 182 23 Prague 8, Czech Republic

ARTICLE INFO

Article history:
Received 3 January 2012
Received in revised form 29 April 2012
Accepted 4 May 2012
Available online 10 May 2012

Keywords:
Ammonium exporters Ato1p, Ato2p and Ato3p
FLIM-photobleaching technique
Homo/hetero di(oligo)mers
Plasma membrane protein interaction
Donor lifetime

ABSTRACT

Each of the three plasma membrane Ato proteins is involved in ammonium signalling and the development of yeast colonies. This suggests that although these proteins are homologous, they do not functionally substitute for each other, but may form a functional complex. Here, we present a detailed combined FRET, FLIM and photobleaching study, which enabled us to detect interactions between Ato proteins found in distinct compartments of yeast cells. We thus show that the proteins Ato1p and Ato2p interact and can form complexes when present in the plasma membrane. No interaction was detected between Ato1p and Ato3p or Ato2p and Ato3p. In addition, using specially prepared strains, we were able to detect an interaction between molecules of the same Ato protein, namely Ato1p–Ato1p and Ato3p–Ato3p, but not Ato2p–Ato2p.

1. Introduction

When growing on solid media, yeast colonies undergo developmental changes accompanied by pH changes to their surroundings from acid-to-alkali and *vice versa*. The ammonia released during the alkali phase acts as a long-range signal, influencing the development of neighbouring colonies [1,2]. Three transmembrane proteins Ato1p (Ycr010p, Ady2p), Ato2p (Ynr002p, Fun34p) and Ato3p (Ydr384p), the expression of which increases sharply during acid-to-alkali colony transition, play an important role in yeast colony development [3]. These proteins belong to the highly conserved Gpr1/Fun34/YaaH family, the members of which are present in prokaryotes and lower eukaryotes (mainly fungi) and their precise function is still unknown. Several findings suggest that Ato proteins play a role in ammonium export, although no direct evidence of their ammonium transporter function has been found so far. i) The production and membrane localisation of Ato proteins correlate with ammonia production and *ATO* gene expression can be prematurely induced by ammonia from an artificial source [4]. ii) The production of Ato proteins is significantly diminished in the colonies of various strains exhibiting a lack of ammonia signalling [5]. iii) Respiration-deficient ρ^0 cells increase their production of Ato3p that is thought to remove an excess of ammonium [6]. Other data indicate that Ato1p and Ato2p are involved in acetic acid sensitivity [7] and Ato1p (but not the other Ato proteins) is involved in acetate uptake in *S. cerevisiae* cells grown in liquid cultures [8].

Although all three Ato proteins were found in the ergosterol-rich fraction of the plasma membrane, each of them exhibits different membrane distribution. Ato1p and Ato3p were found in "raft" patches, differing in their properties. Ato1p, but not Ato3p patch formation is pH-dependent. Ato2p exhibits the most uniform distribution in the membrane [4]. Ato1p and Ato2p are highly homologous (70% amino acid identity), while Ato3p is less similar (33–34% amino acid identity). The absence of any of the three Ato proteins causes a decrease in ammonia production, suggesting that these proteins cannot mutually complement each others' functions [3]. This finding raises the question of whether Ato proteins could function in a cooperative manner, possibly forming complex(es) in the plasma membrane. This possibility is supported by recent data suggesting that the Ato protein orthologue Gpr1p from *Yarrowia lipolytica* may exist in an oligomeric state [7].

FRET (fluorescence resonance energy transfer) is a technique frequently used to confirm protein–protein interactions within living cells [9–11]. Proteins of interest are genetically labelled with fluorescent proteins (FP) forming a FRET pair. If the molecules carrying the

Abbreviations: DRLP, dichroic long pass; FLIM, fluorescence lifetime imaging; FP, fluorescent protein; FRET, fluorescence resonance energy transfer; GM, glycerol medium; LDH, laser diode heads; NA, numerical aperture; PCR, polymerase chain reaction; SPAD, single-photon avalanche diode; TCSPC, time-correlated single-photon counting; tdimer2, tandem dimer of DsRed

* Corresponding author. Tel.: +420 221951721; fax: +420 221951724.
E-mail address: zdenap@natur.cuni.cz (Z. Palková).
[1] Current address: The Institute of Hematology and Blood Transfusion, U Nemocnice 2094/1, 12820 Prague 2, Czech Republic.

0005-2736/$ – see front matter © 2012 Elsevier B.V. All rights reserved.
doi:10.1016/j.bbamem.2012.05.005

fluorophores are close enough (1–10 nm), the excited state energy of the donor can be transferred nonradiatively to the acceptor. Due to that energy transfer, the fluorescence of the acceptor is enhanced at the expense of the fluorescence of the donor. These changes in fluorescence intensities are often used for FRET detection [10,11]. Intensity-based fluorescence measurements are, however, complicated due to bleed-through of the donor fluorescence into an acceptor detection channel in addition to direct excitation of the acceptor fluorescence, which limits the reliability of this approach. The intensity-based measurements can be improved e.g. by methods using acceptor photobleaching, but even here attention should be paid to avoid possible artefacts [12]. Another approach to FRET measurements uses the fact that the quenching of donor fluorescence is also manifested as shortening of its fluorescence lifetime, which can be monitored at microscopic resolution using FLIM (fluorescence lifetime imaging), enabling protein–protein interaction to be localised directly in living cells [13–17]. TCSPC (time-correlated single-photon counting)-based FLIM instruments are preferentially used for this kind of studies [18–20]. In yeast, FLIM–FRET approach based on monitoring of a Cerulean fluorescence donor lifetime (a variant of the cyan fluorescent protein with improved quantum yield [21]) was successfully used to measure interaction of cyclin dependent kinase with B-type cyclins with cytosolic and nuclear localization [22].

Here we combine FRET–FLIM and acceptor photobleaching based FRET to detect interactions between proteins localised to distinct compartments of yeast cells. We show that Ato proteins form complexes in the yeast plasma membrane, in which interaction between specific Ato proteins as well as between the same molecules of a particular Ato protein can occur.

2. Materials and methods

2.1. Strains and media

The strains used in this study (Table 1) are derived from *Saccharomyces cerevisiae* BY4742 (*MATα*, *his3Δ1*, *leu2Δ0*, *lys2Δ0*, *ura3Δ0*) and BY4741 (*MATa*, *his3Δ1*, *leu2Δ0*, *met15Δ0*, *ura3Δ0*), obtained from the EUROSCARF collection. Cells were grown at 28 °C either on GM-BKP agar (1% yeast extract, 3% glycerol, 2% agar, 30 mM $CaCl_2$, 0.01% bromcresol purple, pH 5) for 12–13 days (fully developed alkali phase) or in liquid GM media (1% yeast extract, 3% glycerol, pH 5) for approximately 24 h.

2.2. Construction of strains containing fluorescent fusion proteins

A fluorescent protein (FP) gene-tag (GFP, tdimer2, CFP, Venus) was fused to the appropriate gene directly in the chromosome. A "FP-selection marker" cassette was provided with its 5′-end homologous to the end of the appropriate gene (without a stop codon) and 3′-end homologous to the downstream region of the appropriate gene. For amplification of the cassette, we used the primers for the *ATO1*, *ATO2*, *ATO3*, *JEN1*, *MET17*, *FET3* and *FTR1* genes (Table S1) and the appropriate plasmid as the template. Single-labelled strains were prepared using the pKT209 plasmid (GFP, "green" strains), pKT176 (tdimer2, "red"

Table 1
Strains.

Name	Genotype	Source
BY-Ato1p-GFP	*MATα, his3Δ1, leu2Δ0, lys2Δ0, ura3Δ0, ATO1-yEGFP–CaURA3*	This study
BY-Ato2p-GFP	*MATα, his3Δ1, leu2Δ0, lys2Δ0, ura3Δ0, ATO2-yEGFP–CaURA3*	This study
BY-Ato3p-GFP	*MATα, his3Δ1, leu2Δ0, lys2Δ0, ura3Δ0, ATO3-yEGFP–CaURA3*	This study
BY-Ato1p-tdimer2	*MATα, his3Δ1, leu2Δ0, lys2Δ0, ura3Δ0, ATO1-tdimer2–CaURA3*	Váchová et al., 2009
BY-Ato2p-tdimer2	*MATα, his3Δ1, leu2Δ0, lys2Δ0, ura3Δ0, ATO2-tdimer2–CaURA3*	This study
BY-Ato3p-tdimer2	*MATα, his3Δ1, leu2Δ0, lys2Δ0, ura3Δ0, ATO3-tdimer2–CaURA3*	This study
BY-Ato1p-GFP/Ato2p-tdimer2	*MATα, his3Δ1, leu2Δ0, lys2Δ0, ura3Δ0, ATO1-yEGFP–SpHIS5, ATO2-tdimer2–CaURA3*	This study
BY-Ato1p-GFP/Ato3p-tdimer2	*MATα, his3Δ1, leu2Δ0, lys2Δ0, ura3Δ0, ATO1-yEGFP–SpHIS5, ATO3-tdimer2–CaURA3*	This study
BY-Ato2p-GFP/Ato1p-tdimer2	*MATα, his3Δ1, leu2Δ0, lys2Δ0, ura3Δ0, ATO2-yEGFP–SpHIS5, ATO1-tdimer2–CaURA3*	This study
BY-Ato2p-GFP/Ato3p-tdimer2	*MATα, his3Δ1, leu2Δ0, lys2Δ0, ura3Δ0, ATO2-yEGFP–SpHIS5, ATO3-tdimer2–CaURA3*	This study
BY-Ato3p-GFP/Ato1p-tdimer2	*MATα, his3Δ1, leu2Δ0, lys2Δ0, ura3Δ0, ATO3-yEGFP–SpHIS5, ATO1-tdimer2–CaURA3*	This study
BY-Ato3p-GFP/Ato2p-tdimer2	*MATα, his3Δ1, leu2Δ0, lys2Δ0, ura3Δ0, ATO3-yEGFP–SpHIS5, ATO2-tdimer2–CaURA3*	This study
BY-Ato1p-CFP	*MATα, his3Δ1, leu2Δ0, lys2Δ0, ura3Δ0, ATO1-yECFP–CaURA3*	This study
BY-Ato2p-CFP	*MATα, his3Δ1, leu2Δ0, lys2Δ0, ura3Δ0, ATO2-yECFP–CaURA3*	This study
BY-Ato3p-CFP	*MATα, his3Δ1, leu2Δ0, lys2Δ0, ura3Δ0, ATO3-yECFP–CaURA3*	This study
BY-Ato1p-Venus	*MATα, his3Δ1, leu2Δ0, lys2Δ0, ura3Δ0, ATO1-yEVenus–Kan*	This study
BY-Ato2p-Venus	*MATα, his3Δ1, leu2Δ0, lys2Δ0, ura3Δ0, ATO2-yEVenus–Kan*	This study
BY-Ato3p-Venus	*MATα, his3Δ1, leu2Δ0, lys2Δ0, ura3Δ0, ATO3-yEVenus–Kan*	This study
BY-Ato1p-CFP/Ato2p-Venus	*MATα, his3Δ1, leu2Δ0, lys2Δ0, ura3Δ0, ATO1-yECFP–CaURA3, ATO1-yEVenus–Kan*	This study
BY-Ato2p-CFP/Ato1p-Venus	*MATα, his3Δ1, leu2Δ0, lys2Δ0, ura3Δ0, ATO1-yECFP–CaURA3, ATO1-yEVenus–Kan*	This study
BY-Ato3p-CFP/Ato1p-Venus	*MATα, his3Δ1, leu2Δ0, lys2Δ0, ura3Δ0, ATO1-yECFP–CaURA3, ATO1-yEVenus–Kan*	This study
BY-Ato3p-CFP/Ato2p-Venus	*MATα, his3Δ1, leu2Δ0, lys2Δ0, ura3Δ0, ATO1-yECFP–CaURA3, ATO2-yEVenus–Kan*	This study
BY-Fet3p-GFP	*MATα, his3Δ1, leu2Δ0, lys2Δ0, ura3Δ0, FET3–yEGFP–CaURA3*	This study
BY-Ftr1p-GFP	*MATα, his3Δ1, leu2Δ0, lys2Δ0, ura3Δ0, FTR1–yEGFP–CaURA3*	This study
BY-Fet3p-GFP/Ftr1p-tdimer2	*MATα, his3Δ1, leu2Δ0, lys2Δ0, ura3Δ0, FET3–yEGFP–CaURA3, FTR1–tdimer2–CaURA3*	This study
BY-Fet3p-tdimer2/Ftr1p-GFP	*MATα, his3Δ1, leu2Δ0, lys2Δ0, ura3Δ0, FET3–tdimer2–CaURA3, FTR1–yEGFP–CaURA3*	This study
BY-Jen1p-GFP	*MATα, his3Δ1, leu2Δ0, lys2Δ0, ura3Δ0, JEN1–yEGFP–SpHIS5*	This study
BY-Jen1p-GFP/Ato1p-tdimer2	*MATα, his3Δ1, leu2Δ0, lys2Δ0, ura3Δ0, JEN1–yEGFP–SpHIS5, ATO1–tdimer2–CaURA3*	This study
BY-Jen1p-GFP/Ato2p-tdimer2	*MATα, his3Δ1, leu2Δ0, lys2Δ0, ura3Δ0, JEN1–yEGFP–SpHIS5, ATO2–tdimer2–CaURA3*	This study
BY-Met17p-GFP	*MATα, his3Δ1, leu2Δ0, lys2Δ0, ura3Δ0, MET17–yEGFP–Kan*	This study
BY-Ato1p-GFP (BY4741)	*MATa; his3Δ1; leu2Δ0; met15Δ0; ura3Δ0, ATO1–yEGFP–CaURA3*	This study
BY-Ato2p-GFP (BY4741)	*MATa; his3Δ1; leu2Δ0; met15Δ0; ura3Δ0, ATO2–yEGFP–CaURA3*	This study
BY-Ato3p-GFP (BY4741)	*MATa; his3Δ1; leu2Δ0; met15Δ0; ura3Δ0, ATO3–yEGFP–CaURA3*	This study
BY-Ato1p-GFP/Ato1p-tdimer2	*MATa/MATα; his3Δ1/his3Δ1; leu2Δ0/leu2Δ0; met15Δ0/MET15;LYS2/lys2Δ0; ura3Δ0/ura3Δ0, ATO1–yEGFP–CaURA3/ATO1-tdimer2–CaURA3*	This study
BY-Ato2p-GFP/Ato2p-tdimer2	*MATa/MATα; his3Δ1/ his3Δ1; leu2Δ0/leu2Δ0; met15Δ0/MET15;LYS2/lys2Δ0; ura3Δ0/ura3Δ0, ATO2–yEGFP–CaURA3/ATO2-tdimer2–CaURA3*	This study
BY-Ato3p-GFP/Ato3p-tdimer2	*MATa/MATα; his3Δ1/ his3Δ1; leu2Δ0/ leu2Δ0; met15Δ0/MET15;LYS2/lys2Δ0; ura3Δ0/ura3Δ0, ATO3–yEGFP–CaURA3/ATO3-tdimer2–CaURA3*	This study

strains), pKT174 (CFP, "blue" strains) and pKT103 (Venus, "yellow" strains). Double-labelled strains were prepared using pKT128/pKT176 (GFP–tdimer2, "green–red" strains) and pKT174/pKT103 (CFP–Venus, "blue–yellow" strains). The constructed cassettes were transformed [23] into BY4742 cells and positive transformants were selected either on SD agar medium with auxotrophic supplements or on YPD medium with the appropriate concentration of antibiotic. Correct integration of the cassette was verified by PCR. The diploid strains were constructed by mating (crossing) the BY4741 and BY4742 strains with ATO-GFP and ATO-tdimer2 fusions, respectively.

2.3. Microscopy sample preparation

Cells taken from the inner rim of the colony (Fig. S1) were resuspended in distilled water, spotted onto a cover slip and covered with a rectangular piece of agarose cut out of a thin 0.8% agarose layer. Cells from the liquid culture were washed twice with distilled water before microscopy sample preparation.

2.4. Cell fractionation and GFP detection

Cell lysates from alkali-phase colonies and liquid GM medium, respectively, were prepared [24] and separated to the membrane [4] and soluble fractions (includes also vacuolar lumen). Proteins from each fraction were analysed by SDS-PAGE and subsequent immunoblotting. To detect Ato-GFP and free GFP proteins, we used mouse monoclonal anti-GFP antibody, horseradish peroxidase (HRP) conjugate (Santa Cruz). The Pma1p, marker of plasma membrane, was detected by specific goat anti-Pma1 antibodies (Santa Cruz Biotechnology) in combination with rabbit anti-goat IgG-peroxidase (Sigma) as the secondary antibody [24].

2.5. Fluorescence lifetime imaging

2.5.1. Instrumental setup

We studied two FRET pairs: GFP–tdimer2 and CFP–Venus. Data for both the pairs were acquired with Microtime 200 inverted confocal microscope (PicoQuant, Berlin, Germany) [25]. Donors and acceptors were excited quasi-simultaneously with alternatively pulsing laser beams [26]. The pulsed interleaved excitation (PIE) allows for independent mapping of the acceptor signal, which was used for construction of the saturation curves.

For excitation we used the following excitation wavelengths: 440 nm (LDH-D-C-440) for CFP, 470 nm (LDH-P-C-470) for GFP, and 532 nm (PicoTa) for tdimer2 and Venus. All the used lasers were from Picoquant (Berlin, Germany) providing ~80 ps pulses. When applied in the PIE mode, the repetition rate was 20 MHz for each of the two lasers with the delay between the donor and the acceptor excitation pulse of approximately 25 ns.

The excitation pulses were reflected to the objective (60×, NA = 1.2, Olympus, Hamburg, Germany) with Z442/532 RPC (CFP–Venus) and Z473/532 RPC (GFP–tdimer2) dichroic mirrors (Chroma, Rockingham, VT). In the detection path, the 50-μm pinhole was placed to reduce non-focal fluorescence. Behind the pinhole, a fluorescence signal was split with a 535 DCXC dichroic mirror, and the residual excitation and scattered light were removed with emission filters: 465/40 (CFP), 505/30 (GFP), and 565/40 (Venus and tdimer2). Eventually, the light was focused on two single photon avalanche diodes (SPADs, PDMs, Microphoton Devices, Bolzano, Italy).

Pixel acquisition time was adjusted to acquire the entire image in a reasonably short time (5 min or less) with sufficiently good photon statistics. The laser power (at the back aperture of the objective) kept below 4 μW was chosen to minimise photobleaching and saturation [27]. In the case of the GFP–tdimer pair, the excitation intensity was 3–5 times lower compared to CFP–Venus constructs in order to avoid pile-up effects.

2.5.2. Data acquisition and processing, lifetime analysis

Photon arrival times were stored using fast electronics (Picoharp 300, PicoQuant, Berlin, Germany) in a time-tagged time resolved (TTTR) recording mode. In this mode, arrival time with respect to the previous laser pulse is assigned to every photon event. FLIM images were reconstructed using a robust fitting-free fast-FLIM approach, in which photons' average arrival time is displayed for every given pixel. For regions of interest (plasma membrane, vacuoles), integral decay histograms were calculated and subsequently they were tail-fitted. Since the fluorescence decay of CFP is reported to be bi-exponential [28], our data were fitted with a two-exponential model: $I(t) = A_1\exp(-t/\tau_1) + A_2\exp(-t/\tau_2)$, where τ stands for fluorescence lifetime and A for amplitude of individual contribution. An average lifetime was calculated using the following equation: $\tau_{av} = (A_1 \cdot \tau_1^2 + A_2 \cdot \tau_2^2)/(A_1 \cdot \tau_1 + A_2.\tau_2)$ [29]. A satisfying fit was typically obtained for fluorescence decays counting more than a thousand registered photons in the peak.

2.6. FRET analysis

2.6.1. Half-cell photobleaching approach

First, we measured and imaged fluorescence lifetimes within whole yeast cells so that we could analyse fluorescence lifetimes in their plasma membranes. Then, we photobleached the acceptor in a limited area of a living yeast cell with a strong incident light. Photobleaching was performed by raising the power of the scanning laser to its maximum (200 μW) and by prolonging the illumination time per pixel (typically 4× or 5×). This enabled us to photobleach both acceptors, whether Venus or tdimer2 was used. Finally, we visualised the possible presence of FRET directly by comparing donor lifetimes detected in a photobleached and non-photobleached part of the cell.

2.6.2. Lifetime dependence on acceptor/donor ratio

For interacting proteins, shortening of the donor lifetime depends on the relative amount of acceptor available. The experimentally observed lifetime consists of the non-interacting donor lifetime and the donor lifetime shortened due to FRET. The higher the acceptor-to-donor ratio (R), the shorter the observed lifetime is. The dependence of the observed overall lifetime on R can be fitted with an empirical formula: $\tau_D = \tau_{D0} - \Delta\tau \cdot R/(b + R)$, where τ_{D0} is the lifetime of a non-interacting donor, $\Delta\tau$ is the maximum shift in lifetimes due to FRET, and b is the scaling factor. The lifetime dependence on R was generated from a heterogeneous set of at least 20 fluorescent cells. R was calculated as the amplitude ratio of membrane-integrated decays for the donor and the acceptor.

2.6.3. Fluorescence recovery after photobleaching measurement

Samples for fluorescence recovery after photobleaching measurement (FRAP) were prepared as described above. FRAP analysis was performed using a Leica TCS SP2 AOBS inverted confocal microscope with a 63×1.2 numerical aperture water objective. The 488 argon laser line was used to excite GFP and the fluorescence emission between 500 nm and 550 nm was recorded. Fluorescence intensities in the respective ROIs (background, bleached part of a membrane and control part of a membrane) were recorded in each time-point (two different setups were used: either 3 pre-bleach and 20 post-bleach scans in the interval of 0.5 s or 6 pre-bleach and 60 post-bleach scans in the interval of 5 s were done). At least 8 cells of each strain were measured. The mobile fraction F_m of Ato-GFP proteins was estimated using normalised data (where pre-bleach intensity was assigned a value 1) and the equation $F_m = (I_E - I_0)/(1 - I_0)$, where I_E stands for the end value of the recovered fluorescence intensity and I_0 stands for the first post-bleach fluorescence intensity.

3. Results and discussion

3.1. Fluorophore lifetime is influenced by fusion to particular Ato protein

We used two different pairs of fluorescent donor and acceptor, CFP–Venus [27,30] and GFP–tdimer2 (tandem dimer mutant of dsRed) [31]. We prepared two sets of *S. cerevisiae* strains containing *ATO* genes individually fused with genes coding for the respective fluorescent proteins directly in the chromosome (Table 1). The resulting strains were phenotypically comparable with the parental BY4742 strain, thus confirming that individual Ato proteins with any of the four C-terminal fluorophore tags are fully functional. For all measurements described below, we used cells from 12 to 13-day-old colonies occurring in alkali phase and producing high quantities of Ato proteins.

Using cells containing single Ato proteins labelled with the particular donor fluorophore (CFP or GFP, respectively), we first determined the lifetime of the protein-fluorophore fraction localised to the plasma membrane, i.e. of the fluorophore fused with membrane-localised Ato protein. Fluorescence data were obtained from a large section of the plasma membrane (from at least half of the cell) and the average membrane donor lifetime was calculated. Analysis of smaller yeast membrane areas (e.g. raft patches) was beyond the resolution of the method used. The precise fluorescence lifetime value of either CFP or GFP was dependent on the particular labelled Ato-protein (Fig. 1). Compared to other GFP-labelled membrane proteins used in the study (Jen1p, Fet3p and Ftr1p) and to the GFP-labelled cytosolic Met17p, the lifetime of all GFP-labelled Ato-proteins was shorter (Fig. 1). There are several possible reasons for these differences in FP lifetimes. Trivially, the FP could slightly change its conformation when attached to different proteins and/or in a different probe microenvironment. Another explanation might be pseudo-homo FRET (i.e. FRET between two different emissive forms of the same FPs), which was described for CFP fused with fluorescent proteins crowding inside the cytoplasm [32]. By analogy, the lifetime shortening observed in the yeast membrane can correspond to a local increase in the concentration of any of the Ato proteins. Such a shortening of lifetime attributed to energy migration has already been reported for CFP [33]. The fact that we found a stronger FP lifetime shortening in Ato1p and Ato3p constructs accumulating in the raft patches [4] than in Ato2p supports the hypothesis of lifetime shortening due to FP crowding.

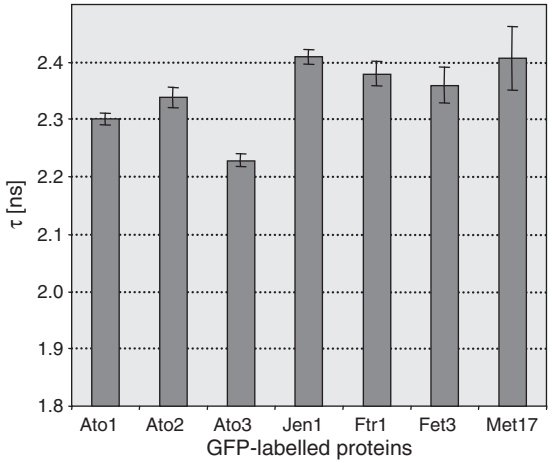

Fig. 1. Lifetimes of GFP fused with different proteins. Lifetimes were measured using BY4742 cells producing a particular protein fused with GFP. The values are the mean of at least 15 cells; bars, SD.

3.2. Ato1p and Ato2p interact in the plasma membrane of cells from alkali-phase colonies

After determining the fluorescence lifetimes of donors fused with each of the three individual Ato proteins, we analysed donor lifetimes in double-labelled cells containing any pair of Ato proteins (Table 1) labelled either with CFP–Venus or GFP–tdimer2 FRET pairs. To avoid possible artefacts caused by variations in the protein level in a distinct cell, we devised the following (Fig. 2, details in Section 2.4 and 2.5) approach: i) measurement of the fluorophore lifetime within the whole cell membrane to control the homogeneity of protein distribution, ii) photo-bleaching of the acceptor molecules in half of a particular cell (the time needed for acceptor photobleaching was 90–120 s depending on cell size) and iii) FLIM measurement in both halves of the cell. When interaction between donor- and acceptor-fused plasma membrane proteins occurs, the fluorescence lifetime of the donor becomes shorter in the non-photobleached compared to the photobleached half of the cell. On the other hand, the donor fluorescence lifetime remains the same in both halves of the cell when proteins do not interact. By using this approach, FRET becomes visible directly in FLIM images of individual cells. As shown in Fig. 3, a significant decrease in donor lifetime was detected in the membrane-localised Ato1p and Ato2p labelled with either of the fluorophore pairs in both combinations (i.e. the donor fluorophore fused with either Ato1p or Ato2p). The average shift in donor lifetime was about 0.15 ns for CFP–Venus labelling (Fig. S2) and 0.25 ns for GFP–tdimer2 labelling of Ato1p–Ato2p proteins (Fig. 3A). In contrast, such a decrease in lifetimes was not observed for combinations of either Ato1p and Ato3p or Ato2p and Ato3p. Photobleaching control experiments using cells where only the donor fluorophore was present did not show any significant difference in donor lifetimes when comparing the photo-bleached and non-photobleached halves of one cell (Fig. S3). This confirmed that donor fluorescence is not artificially affected by the incident light used for the acceptor photobleaching.

As the time window in between the subsequent FLIM measurements was typically 90–120 s, lateral diffusion of bleached proteins during this period of time could influence the measurement. Specifically, it would lead to lowering of the difference between the bleached and unbleached half of the cell. However, proteins of the yeast plasma membrane were shown to exhibit very slow mobility when compared to that of mammalian cells [34,35]. Additionally, Pma1p-GFP, which is an integral membrane protein with ten membrane spanning domains, showed significantly lower mobility when compared to lipid anchored protein Ras2p-GFP [36]. To check the extent of the lateral diffusion of Ato-GFP proteins, we performed a FRAP (fluorescence recovery after photobleaching) experiment taking 5 min. No significant recovery of fluorescence signal was seen neither in 2 min after photobleaching (the maximum time window of the subsequent FLIM measurements) nor in 5 min at the end of the FRAP experiment (Fig. S4). Using normalised FRAP data, mobile fraction F_m of all Ato-GFP was estimated, giving the following values: for Ato1p-GFP $7.3 \pm 2.7\%$, for Ato2p-GFP $8.9 \pm 2.9\%$ and for Ato3p-GFP $5.2 \pm 3.3\%$.

As we have already shown, Ato proteins are targeted to the vacuoles for degradation [4]. Compared to plasma membrane-localised fluorophores fused with Ato, when vacuolar lumen in the cells was selectively photobleached, donor lifetimes were shifted non-specifically by approximately 0.06 ns in each of the strains carrying any pair of fluorescent proteins (Fig. 3B). In addition, the donor lifetimes exhibited a wider range of fluctuations than the lifetimes of donors fused with Ato proteins present in the membrane. The reason is a rapid degradation of Ato proteins in vacuoles, while relatively stable molecules of fluorescent protein in the vacuoles accumulate in high concentrations (Fig. 4) and can potentially interact randomly. These data proved that donor lifetime shifts detected in the membranes reflect specific interaction of particular Ato proteins. Such interaction disappears when an Ato protein part is removed from the fusion protein.

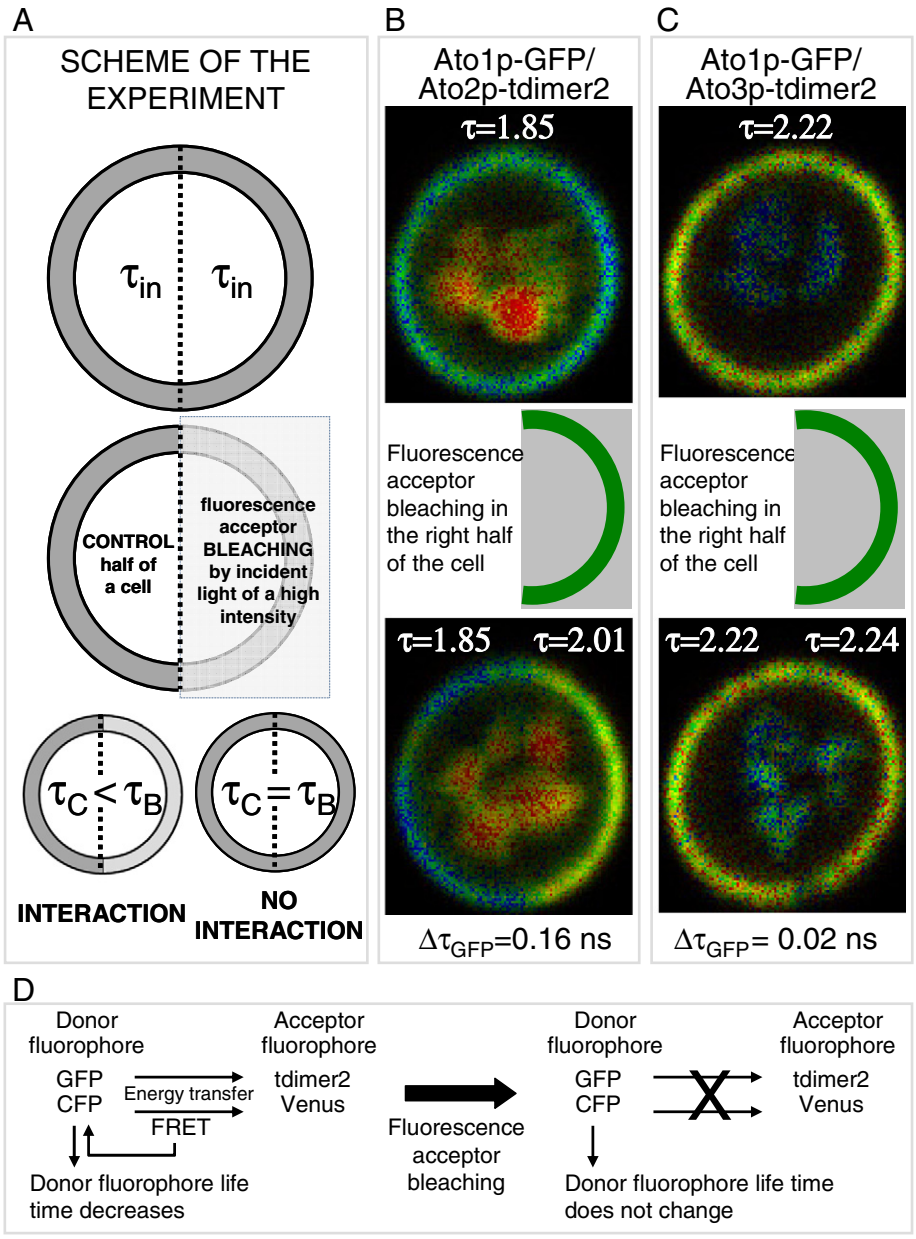

Fig. 2. Measurement of protein–protein interaction in individual living cells. (A) Scheme of the experimental design. Examples of results showing interacting (B) and non-interacting (C) proteins. (D) Principle of FRET using acceptor photobleaching technique.

Each of the fluorophore pairs used has some advantages and disadvantages. The acceptor Venus is easier to photobleach, but exposure to the scanning beam even during standard FLIM imaging can markedly reduce the fluorescence of both Venus and donor CFP. This could cause acceptor photobleaching even during the initial scan, which will reduce FRET and diminish the contrast between photo-bleached and non-photobleached cells. It was observed that the lifetime of CFP-like fluorescent proteins can be shortened due to light exposure [37,38]. For these reasons, the low intensity of an excitation laser beam should be used and repetitive scanning of the same cell should be avoided. In combination with the low quantum yield of the CFP and Venus fluorophores, the fluorescence data thus have to be collected from larger areas of the sample (e.g. larger areas of the plasma membrane). Half-cell photobleaching turned out to be the optimal approach, as it guarantees the registration of CFP lifetimes from areas of comparable size and fluorophore intensity. The quantum yield of GFP and tdimer2 is generally much higher and less affected by the excitation light. This even allows lifetimes to be compared on a whole cell before and after photobleaching, without risking artificial lifetime shortening due to exposure of the fluorophore to incident light during the initial scanning, as mentioned above. Sufficient photobleaching of the tdimer2 acceptor, however, requires higher intensities of incident light. Overall, the GFP–tdimer2 better than the CFP–Venus pair distinguishes differences in lifetimes between interacting and non-interacting fusion proteins. Donor lifetimes measured for the GFP–tdimer2 pair are also less variable than those measured for the CFP–Venus pair because of higher fluorescence signals, enabling a higher accuracy of lifetime calculation.

3.3. Analysis of variation in lifetimes over the cell population confirmed Ato1p–Ato2p interaction

A yeast colony is composed of differentiated cell subpopulations with their own specific gene expression and properties [24,39]. Cells harvested from the colony are therefore heterogeneous and the amount of individual Ato proteins in the plasma membrane of individual cells varies. We therefore applied a second donor FLIM measurement

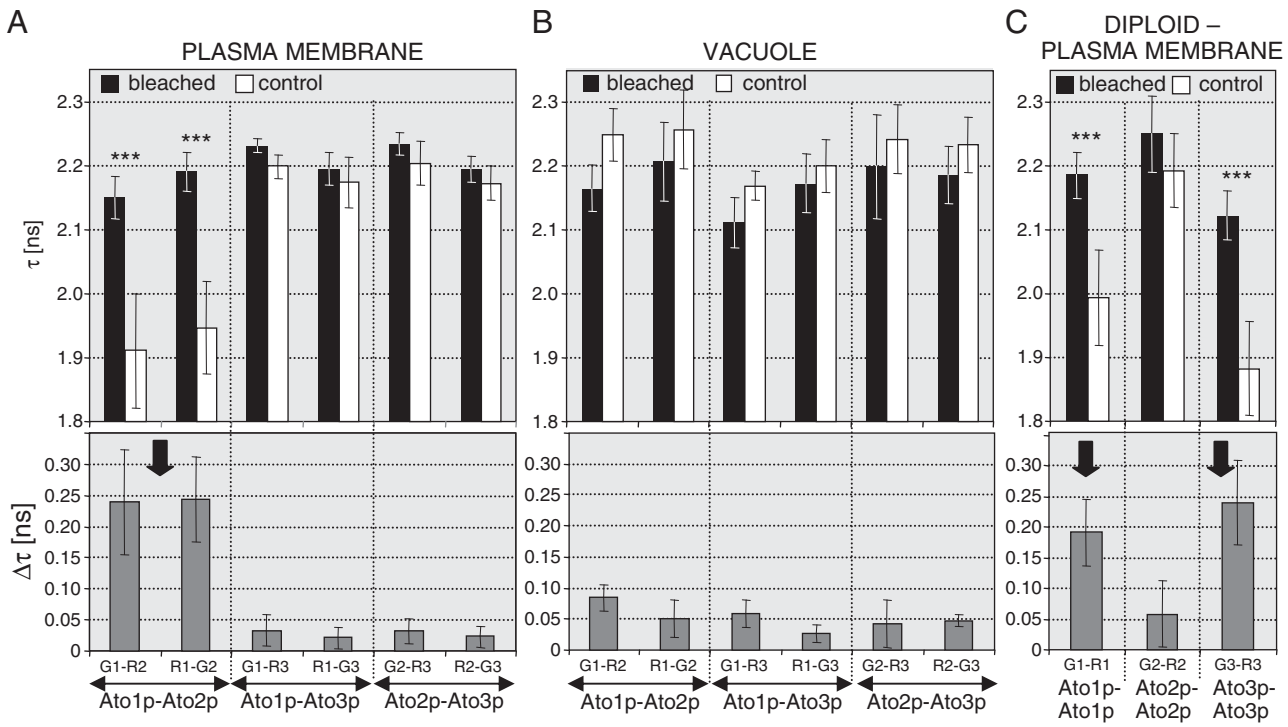

Fig. 3. Interactions of Ato proteins. Donor lifetime measured on FP-labelled proteins in the plasma membrane of double-labelled haploid cells (A), in the vacuole of double-labelled haploid cells (B) and in the plasma membrane of diploid cells with a double-labelled particular Ato protein (C). Vertical arrows indicate interacting proteins. Donor lifetime values before (control) and after (bleached) photobleaching (upper panels), and differences between these two values (lower panels) are shown. G1, G2 and G3, GFP fused with Ato1p, Ato2p and Ato3p, respectively; R1, R2 and R3, tdimer2 fused with Ato1p, Ato2p and Ato3p, respectively. Values from a representative experiment of the three are calculated using at least 5 cells ± SD. Data significance was determined using the one-tailed paired *t* test. *p* values of 0.05 or less were considered statistically significant: $^{***}p<0.005$.

approach, taking into account the varying levels of proteins produced in a heterogeneous yeast population. This approach is based on the assumption that changes in the concentration ratio between acceptor- and donor-fused interacting proteins in the membrane of individual cells will be reflected in the extent of overall donor lifetime shift. With a low concentration of the acceptor relative to the concentration of donor, there is a relatively low number of donor/acceptor pairs in contact and the fluorescence of free donor prevails in the overall fluorescence signal. However when the acceptor is in excess, the portion of donors in contact is much higher, the fluorescence of quenched donors prevails and the mean fluorescence lifetime detected from the membrane is markedly shortened. Thus, when proteins interact, a donor fluorescence lifetime markedly decreases with increased acceptor/donor fluorescence intensity ratio. On the other hand, in the absence of protein–protein interaction, a donor fluorescence lifetime is either independent of acceptor/donor fluorescence intensity ratio or partially shortened due to an excitation transfer occurring at high concentrations of the fused proteins in the membrane (see Section 3.1). However, these situations are clearly distinguishable (see the dependencies measured for interacting and non-interacting proteins in Fig. 6B). Dependence of FRET efficiency on acceptor intensity behaving accordingly to saturable kinetics was previously shown in [40] where CFP and YFP were attached to modified lipids to visualise lipid dynamics in plasma membrane of live Madin–Darby canine kidney cells.

We randomly selected a set of 20–30 yeast cells from the respective population and, in parallel, recorded an overall donor and acceptor fluorescence intensity from the membrane of each cell. We calculated an acceptor/donor intensity ratio, analysed an appropriate donor fluorescence lifetime and fit the dependence of donor lifetimes on the acceptor/donor ratio (R) (see Section 2.5.2). Fig. 5 shows the dependence of lifetimes on the intensity ratios for all combinations of Ato-GFP/Ato-tdimer2 fusion proteins. The plots exhibit saturation

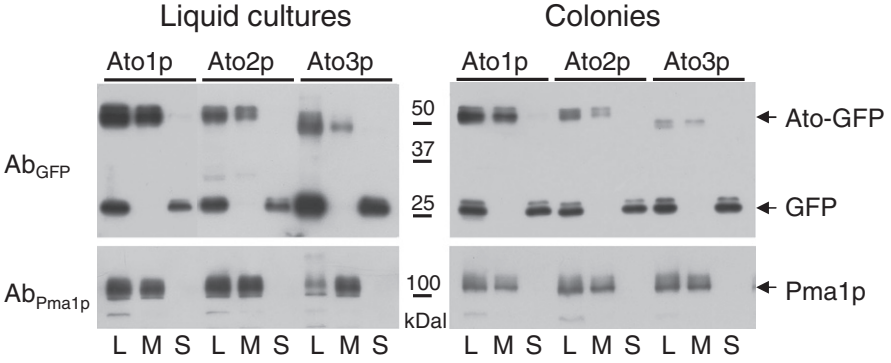

Fig. 4. Ato-GFP fusion proteins and free GFP in plasma membrane and soluble cell fraction. Cell lysates (L), membrane (M) and soluble (S) fractions isolated from cells producing Ato1p-GFP, Ato2p-GFP and Ato3p-GFP, respectively, grown in colonies or liquid cultures. GFP in Ato-GFP fusions or free GFP was detected by anti-GFP antibody (Ab_{GFP}). Pma1p detected by anti-Pma1p antibody (Ab_{Pma1p}) was used as a marker of plasma membrane.

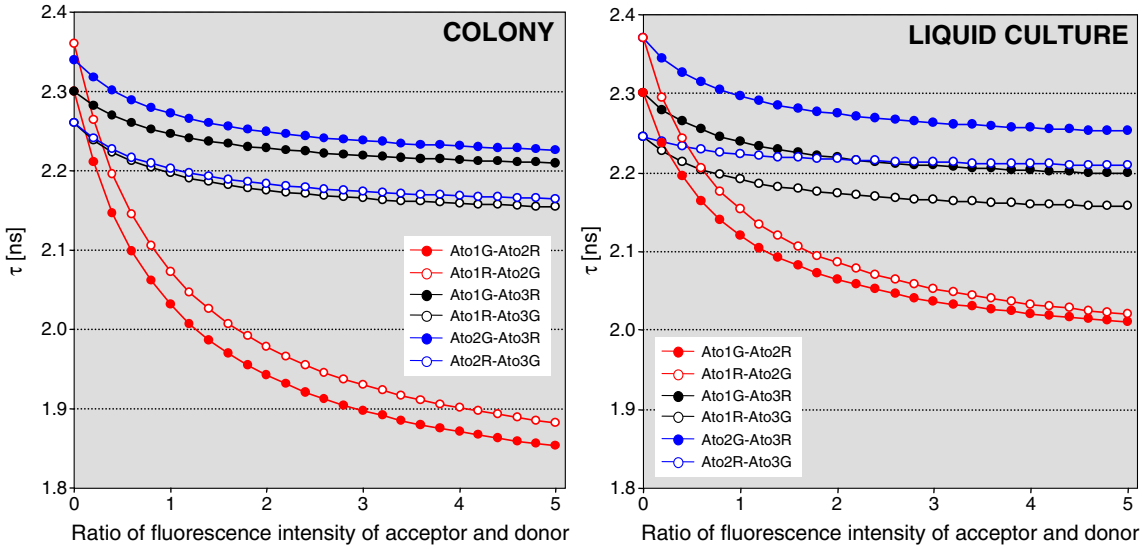

Fig. 5. Determination of protein interactions by measurement of donor lifetime in terms of their dependence on acceptor/donor ratios. Cells were harvested from 12-day-old colonies (left), or from liquid glycerol complete medium (right). G, GFP; R, tdimer2. Real data are shown in Fig. S5 (colonies) and Fig. S6 (liquid cultures).

behaviour, which is in a good agreement with the expectation that the donor molecules should be gradually fully occupied by the interacting acceptor molecules with their increasing concentration. The mean donor lifetime cannot be shorter than the lifetime of an individual donor molecule interacting with the acceptor molecule. The acceptor/donor ratios were in a comparable range for all of our double-fluorophore constructs (Fig. S5). This excludes the possibility that for certain combinations we could only observe FRET stemming from a high concentration of acceptor molecules in the vicinity of donor molecules. In the photo-bleaching-based method, this situation is not taken into account.

The approach presented here is convenient for the detection of new protein–protein interactions in living yeast cells by means of fluorescence lifetime imaging. It avoids the negative impact of natural variation in cell populations (that is often present in biological samples) on the result of FRET measurement when only a randomly chosen individual cell is analysed. In contrast, it takes advantage of this variability and avoids the necessity of acceptor photobleaching. As for Ato proteins, this approach fully confirmed the specific Ato1p–Ato2p interaction observed by the photobleaching method (see Section 3.2).

3.4. Ato1p and Ato3p form homodimers in the membrane

Differences in the lifetime of a donor fluorophore fused with individual Ato proteins (see above) together with the formation of Ato raft patches observed previously [4] raised the question of whether molecules of a particular Ato protein are able to mutually interact. To analyse this possibility, we developed an approach based on the donor FLIM measurement of diploid yeast strains containing the two copies of the same *ATO* gene labelled differently (with a donor and acceptor fluorophore pair) in the two paired chromosomes. To achieve this, we prepared three diploid strains (Ato1p-GFP/Ato1p-tdimer2, Ato2p-GFP/Ato2p-tdimer2, Ato3p-GFP/Ato3p-tdimer2) and measured individual Ato protein interactions using the half-cell photobleaching method (see Section 3.2). As shown in Fig. 3C, a significant decrease in donor lifetime was detected with Ato1p and Ato3p diploids, while the difference between the photobleached and non-photobleached half of the cell was not significant in Ato2p diploids. Ato1p and Ato3p are thus able to form homodimers or homooligomers in the yeast plasma membrane.

3.5. The reliability of approaches was tested using proteins exhibiting a known interaction

To confirm the functionality of these established FLIM approaches, proteins with a known interaction were examined. We chose multicopper oxidase Fet3p and iron permease Ftr1p [41] which physically interact and which were shown to exhibit positive FRET [42]. Both these proteins are involved in high-affinity Fe^{II} uptake and are thought to form heterodimeric or higher-order oligomeric complexes in the yeast plasma membrane [43]. We analysed cells producing Fet3p and Ftr1p proteins labelled with GFP and tdimer2 fluorophores by both approaches. We measured GFP donor lifetimes in the membranes of a representative set of cells to gauge their dependence on the acceptor/donor fluorophore ratio (Fig. 6B) and we examined the changes in donor fluorophore lifetime after photobleaching (Fig. 6A). Both results clearly confirmed a Fet3p–Ftr1p interaction (Fig. 6).

As a negative control, we used the Jen1p protein, involved in lactate uptake [44]. This protein is produced in the cells of GM-grown liquid cultures together with Ato proteins, but there is no structural or functional reason to presume a physical interaction between this protein and any of the Ato proteins. The absence of a detectable interaction between Jen1p-GFP and Ato1p-tdimer2, as well as between Jen1p-GFP and Ato2p-tdimer2 was confirmed by lifetime measurement of the donor fluorophore (Fig. 6). In parallel, we monitored donor lifetime changes in cells containing labelled Ato1p and Ato2p proteins, which revealed an Ato1p–Ato2p interaction, even in cells growing in liquid GM (Fig. 5).

4. Conclusions

Here we present two approaches for monitoring protein–protein interaction in yeast cells and, particularly, in distinct cellular compartments. The measurement of donor lifetime without and after photobleaching enables protein–protein interaction monitoring in one cell, thus eliminating possible artefacts caused by unequal production of the proteins in different cells. This is particularly useful when a differentiated cell population is analysed and a particular protein–protein interaction needs to be correlated with a particular cell function. In addition, by using this approach, differences in protein–protein interaction in different cellular compartments can be characterised. Correlating fluorophore ratios with donor fluorophore lifetimes in individual

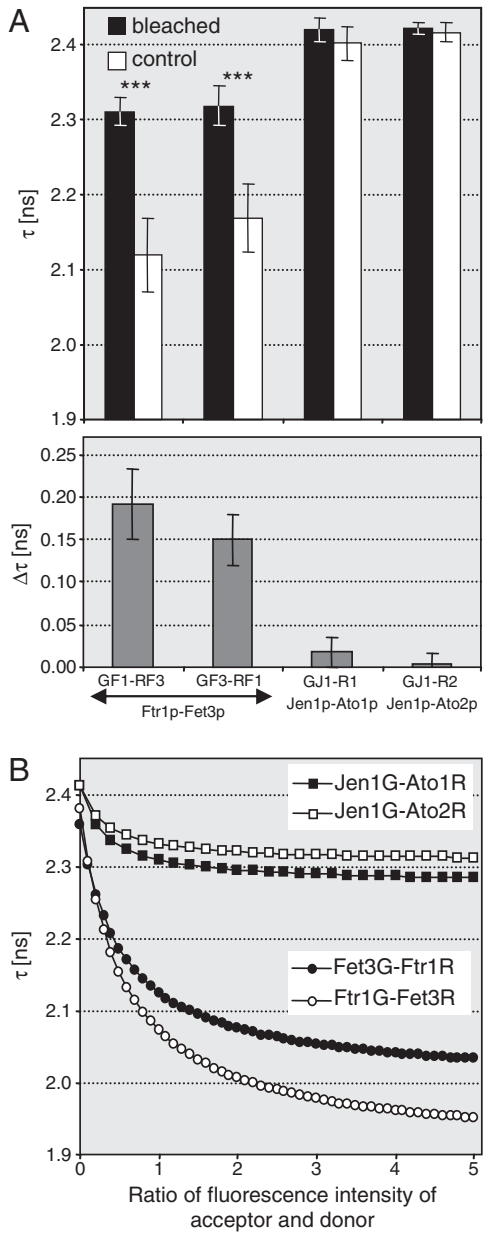

Fig. 6. Measurement of protein–protein interaction using interacting and non-interacting control proteins. (A) Donor lifetime values before and after photobleaching (upper panels), and the difference between these two values (lower panels) are shown. (B) Dependence of donor lifetimes on acceptor/donor ratios. GF1, GF3 and GJ1, Ftr1p, Fet3p and Jen1p fused with GFP, respectively; RF1, RF3, R1 and R2, Ftr1p, Fet3p, Ato1p and Ato2p fused with tdimer2, respectively. Values from a representative experiment of the three are calculated from at least 5 cells ± SD. Data significance was determined using the one-tailed paired *t* test. *p* values of 0.05 or less were considered statistically significant: $^{***}p<0.005$.

cells proved to be useful for monitoring the overall interaction over the whole cell population, composed of cells with various ratios of the production of both proteins. Both acceptor photobleaching-based approach and acceptor/donor intensity ratio approach led to the same results.

Using these approaches, we show that the proteins Ato1p and Ato2p can physically interact when present in the membrane of yeast cells, probably forming complexes. In addition, we show that Ato1p and Ato3p with non-uniform distribution in the membrane [4] can form homodimers and/or oligomers. Neither an interaction between Ato1p and Ato3p, nor between Ato2p and Ato3p, nor homodimerization of Ato2p that exhibits dispersed plasma membrane localisation was observed using our approach. Molecular interaction between these proteins, however, cannot be entirely excluded. These results fully support our hypothesis that Ato proteins form complex(es) and are in accordance with our previous findings that each of the three Ato proteins is necessary for sufficient ammonia production and healthy development of yeast colonies [3]. One can speculate that homo-Ato1p- or Ato3p-complexes are formed within the membrane raft microdomain patches. Of those proteins, only Ato1p that is (in contrast to Ato3p) able to change membrane distribution according to the extracellular pH [4] can interact with Ato2p monomers that are dispersed in the membrane.

Acknowledgements

The authors are grateful to M. Hof for valuable comments on the manuscript. This study was supported by grants from the Grant Agency of the Czech Republic (204/08/0718) and from the Ministry of Education (LC06063, LC531 and MSM0021620858), GAUK 261214, UNCE 204013, RVO 61388971 and by the Howard Hughes Medical Institute International Research Award (#55005623 to Z.P.).

Appendix A. Supplementary data

Supplementary data to this article can be found online at http://dx.doi.org/10.1016/j.bbamem.2012.05.005.

References

[1] Z. Palkova, B. Janderova, J. Gabriel, B. Zikanova, M. Pospisek, J. Forstova, Ammonia mediates communication between yeast colonies, Nature 390 (1997) 532–536.
[2] Z. Palkova, J. Forstova, Yeast colonies synchronise their growth and development, J. Cell Sci. 113 (2000) 1923–1928.
[3] Z. Palkova, F. Devaux, M. Ricicova, L. Minarikova, S. Le Crom, C. Jacq, Ammonia pulses and metabolic oscillations guide yeast colony development, Mol. Biol. Cell 13 (2002) 3901–3914.
[4] M. Ricicova, H. Kucerova, L. Vachova, Z. Palkova, Association of putative ammonium exporters Ato with detergent-resistant compartments of plasma membrane during yeast colony development: pH affects Ato1p localisation in patches, Biochim. Biophys. Acta 1768 (2007) 1170–1178.
[5] L. Vachova, F. Devaux, H. Kucerova, M. Ricicova, C. Jacq, Z. Palkova, Sok2p transcription factor is involved in adaptive program relevant for long term survival of *Saccharomyces cerevisiae* colonies, J. Biol. Chem. 279 (2004) 37973–37981.
[6] N. Guaragnella, R.A. Butow, ATO3 encoding a putative outward ammonium transporter is an RTG-independent retrograde responsive gene regulated by *GCN4* and the Ssy1–Ptr3–Ssy5 amino acid sensor system, J. Biol. Chem. 278 (2003) 45882–45887.
[7] M. Gentsch, M. Kuschel, S. Schlegel, G. Barth, Mutations at different sites in members of the Gpr1/Fun34/YaaH protein family cause hypersensitivity to acetic acid in *Saccharomyces cerevisiae* as well as in *Yarrowia lipolytica*, FEMS Yeast Res. 7 (2007) 380–390.
[8] S. Paiva, F. Devaux, S. Barbosa, C. Jacq, M. Casal, Ady2p is essential for the acetate permease activity in the yeast *Saccharomyces cerevisiae*, Yeast 21 (2004) 201–210.
[9] S. Shibasaki, K. Kuroda, H. Duc Nguyen, T. Mori, W. Zou, M. Ueda, Detection of protein–protein interactions by a combination of a novel cytoplasmic membrane targeting system of recombinant proteins and fluorescence resonance energy transfer, Appl. Microbiol. Biotechnol. 70 (2006) 451–457.
[10] B. Camuzeaux, C. Spriet, L. Heliot, J. Coll, M. Duterque-Coquillaud, Imaging Erg and Jun transcription factor interaction in living cells using fluorescence resonance energy transfer analyses, Biochem. Biophys. Res. Commun. 332 (2005) 1107–1114.
[11] E.A. Jares-Erijman, T.M. Jovin, FRET imaging, Nat. Biotechnol. 21 (2003) 1387–1395.
[12] T.S. Karpova, C.T. Baumann, L. He, X. Wu, A. Grammer, P. Lipsky, G.L. Hager, J.G. McNally, Fluorescence resonance energy transfer from cyan to yellow fluorescent protein detected by acceptor photobleaching using confocal microscopy and a single laser, J. Microsc. 209 (2003) 56–70.
[13] L. Albertazzi, D. Arosio, L. Marchetti, F. Ricci, F. Beltram, Quantitative FRET analysis with the EGFP–mCherry fluorescent protein pair, Photochem. Photobiol. 85 (2009) 287–297.
[14] D. Lleres, S. Swift, A.I. Lamond, Detecting protein–protein interactions in vivo with FRET using multiphoton fluorescence lifetime imaging microscopy (FLIM), Curr. Protoc. Cytom. (2007) (Chapter 12, Unit12 10).
[15] H. Wallrabe, A. Periasamy, Imaging protein molecules using FRET and FLIM microscopy, Curr. Opin. Biotechnol. 16 (2005) 19–27.
[16] F. Festy, S.M. Ameer-Beg, T. Ng, K. Suhling, Imaging proteins in vivo using fluorescence lifetime microscopy, Mol. Biosyst. 3 (2007) 381–391.
[17] J.A. Levitt, D.R. Matthews, S.M. Ameer-Beg, K. Suhling, Fluorescence lifetime and polarization-resolved imaging in cell biology, Curr. Opin. Biotechnol. 20 (2009) 28–36.

[18] R.R. Duncan, A. Bergmann, M.A. Cousin, D.K. Apps, M.J. Shipston, Multi-dimensional time-correlated single photon counting (TCSPC) fluorescence lifetime imaging microscopy (FLIM) to detect FRET in cells, J. Microsc. 215 (2004) 1–12.
[19] W. Becker, A. Bergmann, M.A. Hink, K. Konig, K. Benndorf, C. Biskup, Fluorescence lifetime imaging by time-correlated single-photon counting, Microsc. Res. Tech. 63 (2004) 58–66.
[20] W. Becker, A. Bergmann, C. Biskup, Multispectral fluorescence lifetime imaging by TCSPC, Microsc. Res. Tech. 70 (2007) 403–409.
[21] M.A. Rizzo, G.H. Springer, B. Granada, D.W. Piston, An improved cyan fluorescent protein variant useful for FRET, Nat. Biotechnol. 22 (2004) 445–449.
[22] G. Schreiber, M. Barberis, S. Scolari, C. Klaus, A. Herrmann, E. Klipp, Unraveling interactions of cell cycle-regulating proteins Sic1 and B-type cyclins in living yeast cells: a FLIM-FRET approach, FASEB J. 26 (2012) 546–554.
[23] R.D. Gietz, R.H. Schiestl, A.R. Willems, R.A. Woods, Studies on the transformation of intact yeast cells by the LiAc/SS-DNA/PEG procedure, Yeast 11 (1995) 355–360.
[24] L. Vachova, H. Kucerova, F. Devaux, M. Ulehlova, Z. Palkova, Metabolic diversification of cells during the development of yeast colonies, Environ. Microbiol. 11 (2009) 494–504.
[25] M. Wahl, F. Koberling, M. Patting, H. Rahn, R. Erdmann, Time-resolved confocal fluorescence imaging and spectroscopy system with single molecule sensitivity and sub-micrometer resolution, Curr. Pharm. Biotechnol. 5 (2004) 299–308.
[26] B.K. Muller, E. Zaychikov, C. Brauchle, D.C. Lamb, Pulsed interleaved excitation, Biophys. J. 89 (2005) 3508–3522.
[27] M. Millington, G.J. Grindlay, K. Altenbach, R.K. Neely, W. Kolch, M. Bencina, N.D. Read, A.C. Jones, D.T. Dryden, S.W. Magennis, High-precision FLIM-FRET in fixed and living cells reveals heterogeneity in a simple CFP-YFP fusion protein, Biophys. Chem. 127 (2007) 155–164.
[28] A. Villoing, M. Ridhoir, B. Cinquin, M. Erard, L. Alvarez, G. Vallverdu, P. Pernot, R. Grailhe, F. Merola, H. Pasquier, Complex fluorescence of the cyan fluorescent protein: comparisons with the H148D variant and consequences for quantitative cell imaging, Biochemistry 47 (2008) 12483–12492.
[29] J.R. Lakowicz, Principles of Fluorescence Spectroscopy, 3rd ed. Springer, New York, 2006.
[30] M.A. Rizzo, G. Springer, K. Segawa, W.R. Zipfel, D.W. Piston, Optimization of pairings and detection conditions for measurement of FRET between cyan and yellow fluorescent proteins, Microsc. Microanal. 12 (2006) 238–254.
[31] X. Yang, P. Xu, T. Xu, A new pair for inter- and intra-molecular FRET measurement, Biochem. Biophys. Res. Commun. 330 (2005) 914–920.
[32] R. Grailhe, F. Merola, J. Ridard, S. Couvignou, C. Le Poupon, J.P. Changeux, H. Laguitton-Pasquier, Monitoring protein interactions in the living cell through the fluorescence decays of the cyan fluorescent protein, Chemphyschem 7 (2006) 1442–1454.
[33] S.V. Koushik, S.S. Vogel, Energy migration alters the fluorescence lifetime of Cerulean: implications for fluorescence lifetime imaging Forster resonance energy transfer measurements, J. Biomed. Opt. 13 (2008) 031204.
[34] J. Valdez-Taubas, H.R. Pelham, Slow diffusion of proteins in the yeast plasma membrane allows polarity to be maintained by endocytic cycling, Curr. Biol. 13 (2003) 1636–1640.
[35] S. Ganguly, P. Singh, R. Manoharlal, R. Prasad, A. Chattopadhyay, Differential dynamics of membrane proteins in yeast, Biochem. Biophys. Res. Commun. 387 (2009) 661–665.
[36] K.C. Vinnakota, D.A. Mitchell, R.J. Deschenes, T. Wakatsuki, D.A. Beard, Analysis of the diffusion of Ras2 in *Saccharomyces cerevisiae* using fluorescence recovery after photobleaching, Phys. Biol. 7 (2010) 026011.
[37] B. Hoffmann, T. Zimmer, N. Klocker, L. Kelbauskas, K. Konig, K. Benndorf, C. Biskup, Prolonged irradiation of enhanced cyan fluorescent protein or Cerulean can invalidate Forster resonance energy transfer measurements, J. Biomed. Opt. 13 (2008) 031205.
[38] M. Tramier, M. Zahid, J.C. Mevel, M.J. Masse, M. Coppey-Moisan, Sensitivity of CFP/YFP and GFP/mCherry pairs to donor photobleaching on FRET determination by fluorescence lifetime imaging microscopy in living cells, Microsc. Res. Tech. 69 (2006) 933–939.
[39] L. Vachova, O. Chernyavskiy, D. Strachotova, P. Bianchini, Z. Burdikova, I. Fercikova, L. Kubinova, Z. Palkova, Architecture of developing multicellular yeast colony: spatio-temporal expression of Ato1p ammonium exporter, Environ. Microbiol. 11 (2009) 1866–1877.
[40] D.A. Zacharias, J.D. Violin, A.C. Newton, R.Y. Tsien, Partitioning of lipid-modified monomeric GFPs into membrane microdomains of live cells, Science 296 (2002) 913–916.
[41] R. Stearman, D.S. Yuan, Y. Yamaguchi-Iwai, R.D. Klausner, A. Dancis, A permease–oxidase complex involved in high-affinity iron uptake in yeast, Science 271 (1996) 1552–1557.
[42] A. Singh, S. Severance, N. Kaur, W. Wiltsie, D.J. Kosman, Assembly, activation, and trafficking of the Fet3p.Ftr1p high affinity iron permease complex in *Saccharomyces cerevisiae*, J. Biol. Chem. 281 (2006) 13355–13364.
[43] E.Y. Kwok, S. Severance, D.J. Kosman, Evidence for iron channeling in the Fet3p–Ftr1p high-affinity iron uptake complex in the yeast plasma membrane, Biochemistry 45 (2006) 6317–6327.
[44] M. Casal, S. Paiva, R.P. Andrade, C. Gancedo, C. Leao, The lactate–proton symport of *Saccharomyces cerevisiae* is encoded by *JEN1*, J. Bacteriol. 181 (1999) 2620–2623.